Battery Tray Design Report

1) Functions, Objective and Constraints (FOCs)

Functions	• Handle the weight of the battery (350kg) under normal use cases. • Secures the battery safely and protects it from external harm.
Objectives	• Minimise cost and mass
Constraints (Numerical constraints, non-negotiable conditions that must be met)	• Must be able to contain 1000x2000x100mm battery pack. • Four locating pins 100mm and 50mm diameter are situated 1500mm apart in the X direction, 1200mm apart in Y direction. • The tray must totally isolate the battery from the external environment. • The tray must be a good conductor to be able to dissipate heat produced by the battery (Battery operating environment -20°C to 60°C) • Must be durable to withstand any forces that acts on the tray. (52kN at bank turns). Providing a safety factor of at least 2. • Lifetime of at least 5 years under extensive uses: 1. Corrosion and rust resistance (able to handle pH 1 of H_2SO_4) 2. High fatigue strength • 6 attaching points. • Commercially viable • The design must allow easy access to bolts when replacing the battery and the tray.
Free Variables (What can be changed?)	• Location of holes • Tray dimensions (shape, size, thickness) • Material selection

2) Material and Manufacturing Process Selections

Material Selection

Firstly, some materials are filtered out to satisfy the constraints. Then, 6 material performances index (MPIs) are derived and used to create graphs with surface trade-off lines.

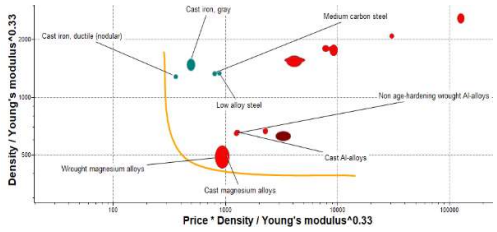

Figure 1: $\frac{\rho}{E^{0.33}}$ *vs* $\frac{C_m\rho}{E^{0.33}}$

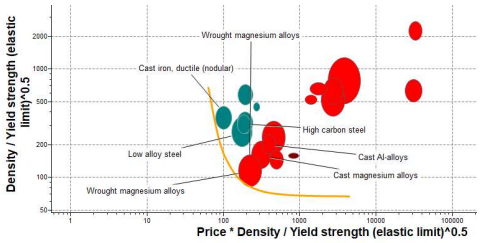

Figure 2: $\frac{\rho}{\sigma_y^{0.5}}$ *vs* $\frac{C_m\rho}{\sigma_y^{0.5}}$

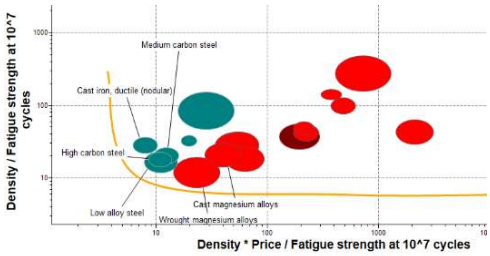

Figure 3: $\frac{\rho}{\sigma_e}$ *vs* $\frac{C_m\rho}{\sigma_e}$

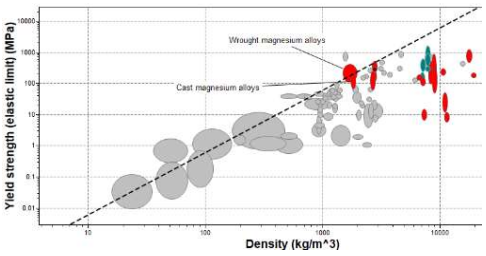

Figure 4: σ_y *vs* ρ

Based on these graphs, 4 materials were found to be suitable including: cast iron (ductile), cast magnesium alloys, low alloy steels and wrought magnesium-alloys. Although the iron and steel are cheaper, we decided to use magnesium alloys as they have higher MPI values of strength with respect to density, which we prioritise over cost due to its effect on the performance of the cars and the force acting on the tray due to gravity. Additionally, magnesium alloys are resistant to water and acid, providing protection against rust, acid rain and rural atmosphere.

Manufacturing Process

Applying the limits of non-ferrous metals, since magnesium alloys are non-ferrous, a mass range of 50-100kg is estimated for the weight of the tray, range of section thickness between 5 mm and 15 cm as it is the planned thickness of the walls, it must have a smooth surface roughness and it must be solid 3D. This leads to 2 primary shaping processes: forging and high pressure die casting.

Upon further research, forging will be selected due to its higher range of section thickness, larger mass range and lower cost for 10,000 batch size. A secondary manufacturing process, like milling, can be implemented to increase its accuracy or fix the tray after casting. Due to this selection, wrought magnesium alloy is chosen instead of cast magnesium alloy.

Figure 5

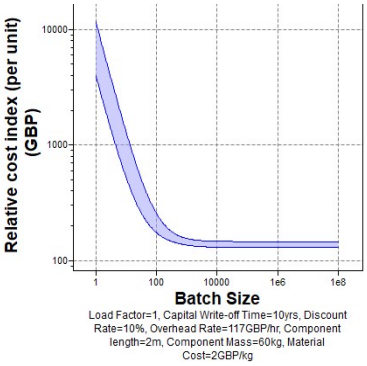

From the cost analysis for forging shown in Figure 5, the cost of a tray is estimated to be £150 as the batch size would be approximately 10000 units. Even though it is on the expensive side, it will be benefited in terms of electricity bills and the environment in the long run.

Surface Treatment

The selected material is cast magnesium alloy, which is not durable against pure oxygen gases, it could be oxidised in a high-temperature environment produced by the battery. Therefore, a surface treatment is needed to be applied to the material to extend the material's lifetime. Furthermore, other desirable properties such as high hardness and good thermal conduction are essential to ensure a safe working condition for the battery. The only suitable surface treatment for a potentially complex battery container shape is electroless plating.

Sustainability

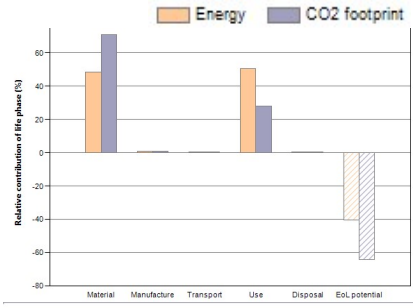

Figure 6

ECO-Audit tool is used to analyse the performance of the tray based on wrought magnesium alloy and forging throughout its lifetime of 10 years. Carbon dioxide (CO_2) production and energy consumption will be looked in each area: material production, manufacturing, transport, and use.

Phase	Energy (MJ)	Energy (%)	CO2 footprint (kg)	CO2 footprint (%)
Material	1.74e+04	48.3	2.42e+03	70.9
Manufacture	378	1.1	28.3	0.8
Transport	23.1	0.1	1.66	0.0
Use	1.81e+04	50.5	962	28.1
Disposal	42	0.1	2.94	0.1
Total (for first life)	**3.6e+04**	**100**	**3.42e+03**	**100**
End of life potential	-1.45e+04		-2.2e+03	

Figure 7

From the data, two main concerns are material production and usage as they tend to produce a large amount of CO_2 and consume a lot of energy. However, the graph suggests that if the material is recycled, then a large amount of energy and CO_2 footprint can be recovered. The data also confirms that material is essential to the environmental factor. A material with a high strength per unit mass is recommended to lower the mass of the design as much as possible to reduce the vehicle energy consumption.

Cast irons and low alloy steels have a lower strength per unit density than that of wrought magnesium alloys of about 15-25%. This means the design needs to be about 1.13-1.25 times heavier to achieve the same required strength. If these materials were chosen, the vehicle would consume about 2-5 giga-Jules more energy than wrought magnesium alloy over its lifetime. Based on the UK electricity bill (Statista Research Department, 2021), using these materials will cost more (around £110-£280) than the wrought magnesium tray. Thus, we conclude that using wrought magnesium alloy is more economically viable in long run and more environmentally friendly in long run.

3) <u>Analytical solutions: Load Cases</u>

Notation: $\boldsymbol{P_{ID}}$ (P = parameter being analysed, I = item or body being analysed, D = direction)

EV Model: Porsche Taycan Turbo S[3]	
Maximum forward acceleration	$11.6\ ms^{-2}$
Top speed	$260\ kmh^{-1}$

General road cases	
Maximum inclined angle (α)	22°
Radius of curvature (bank turn, R)	$10.7\ m$[2]

Load Cases	Battery		Tray		Load on tray surfaces
	Free body diagram	Kinetic diagram	Free body diagram	Kinetic diagram	
Constant velocity ($0 \leq \alpha \leq 22°$)	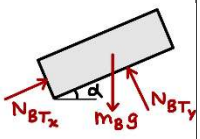		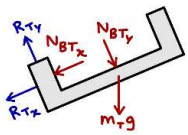	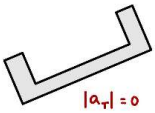	**Case 1:** $\alpha = 0°$ $N_{BTy} = 3433.5N$ $N_{BTx} = 0\ N$ **Case 2:** $\alpha = 22°$ $N_{BTy} = 3183.5N$ $N_{BTx} = 1286.2\ N$
Accelerating /decelerating ($0 \leq \alpha \leq 22°$)	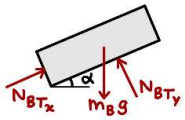	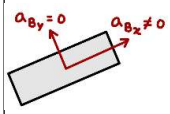	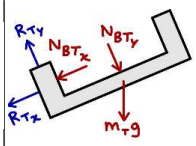	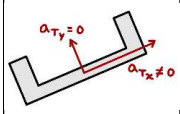	**Case 3:** $\alpha = 0°$ $N_{BTy} = 3433.5N$ $N_{BTx} = 4060\ N$ **Case 4:** $\alpha = 22°$ $N_{BTy} = 3183.5N$ $N_{BTx} = 5346.2\ N$
Cornering (constant velocity 30km/h, R=6m)	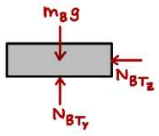	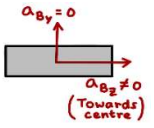	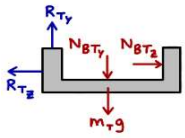		**Case 5:** $N_{BTy} = 3433.5N$ $N_{BTz} = 4038.5\ N$
Bank turn ($\alpha \leq 22°$) at 150 km/h constant)	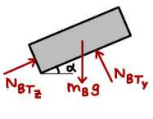	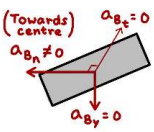	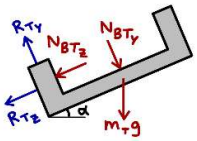	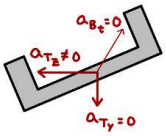	**Case 6:** $N_{BTy} = 24456.9N$ $N_{BTz} = -51367.3N$

4) Computational Solutions and Analysis (FEA, CAD and critiques reference to the boundary conditions)

i) Initial Design

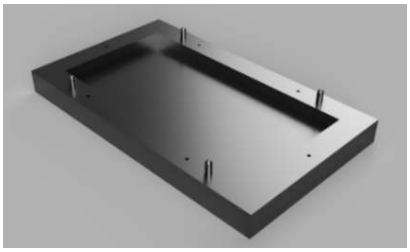

Figure 8

The design process begun with a block shape that has a slot for battery housing, which aimed to provide a protective layer and secure the battery safely. Furthermore, holes for the provisional mounting points and some constrain structures such as the 4 location pins as shown in Figure 8. The mounting points are applied with the fix constrains and the location pins are applied with limited movement in x and y direction. This design underwent a topology optimisation simulation to find the critical load path within the structure. The result is shown in Figure 9; this led us to the general shape of the battery tray.

The critical load path found was the underlying pin for the first iteration of design.

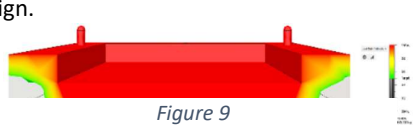

Figure 9

ii) Modified Designs Analysis

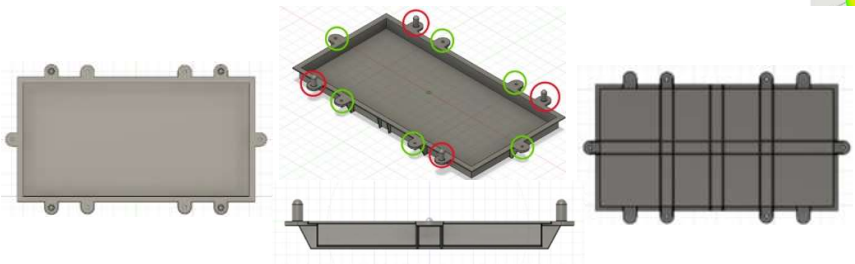

Figure 10: Top view(left), Isometric view(top), Front view(bottom), Bottom view(right)

From the isometric view in Figure 10, the first design iteration includes 4 location pins (red circle), 6 holes for bolts (green circle) and rib structures underneath the tray. The same six load cases are applied to the tray and we found that the load case 6, turning on a 22° bank angle, yields the highest stress on the tray.

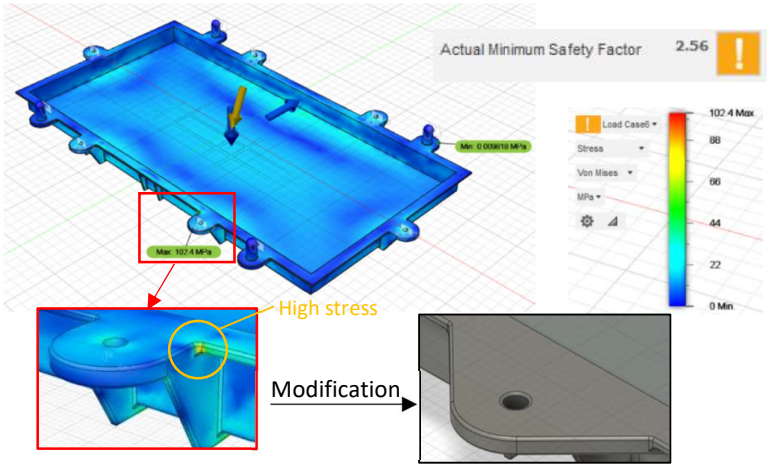

Figure 11: Simulated result for the modified design (first iteration) for case 6

In the close-up view around one of the bolt holes in Figure 11, the joint is shown to be handling the **highest stress of 102.4 MPa,** thus a chamfer is added connecting the circular platform where the bolt hole is located to the sides of the tray in the second design iteration. The reason behind this is because, the possibility of failure of the joints mentioned can be eliminated, thus analysis on the main body holding the battery can be more accurate.

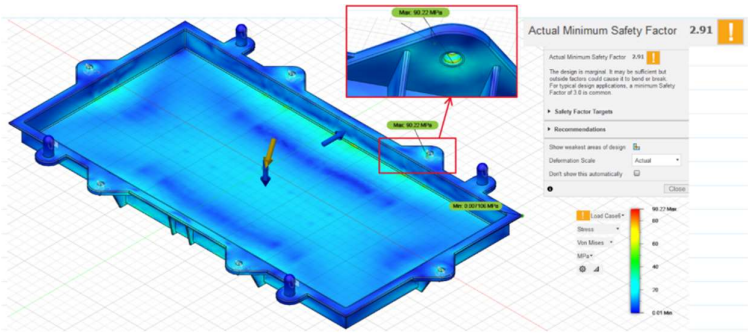

Figure 12: Simulated result for the modified design (second iteration) for case 6

The stress distribution of the modified design (Figure 12) shows the elimination of high stress on the joints; however, the inside surface of the bolt hole now experiences the **highest stress (90.22 MPa)** due to reaction force as the battery pushes on the side of the tray (away from the centre of turning curvature), causing the bolt needing to support not just the vertical (y-direction) load but also the side load (z-direction). However, the **safety factor (2.91)** increased comparing to the previous cases and it is still within expectations (of safety factor = 2) as the load cases simulated are in extreme conditions.

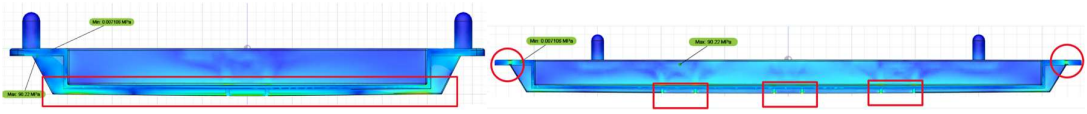

Figure 13: Front cross-section view (left), Side cross-section view (right)

The cross-section views of the tray (Figure 13) show that stresses are mostly distributed at the ribs under the tray (red rectangles) rather than the tray body. Hence, failure will be expected from the ribs structure before the tray body, giving us extra protection in all load cases. In the red circles, stress is high due to the support forces from the bolts. In our analysis, we assume that standard alloy steel thread-locking socket head screws, with tensile strength of 170,000 psi (1.17 GPa) (McMaster-Carr, 2021), are used while our maximum stress is 90.22 MPa.

iii) Shape Optimisation (50% mass preservation)

Bolt holes and location pins are preserved as we perform shape optimisation as we cannot allow any fracture at these parts. From the results of shape optimisation, we can conclude that the most critical regions that are to be preserved include the rectangle tray body and surfaces leading to the support components (location pins and bolts). As the shape optimisation show that we can removed the ribs structure, we would run our **generative design without the ribs structure.**

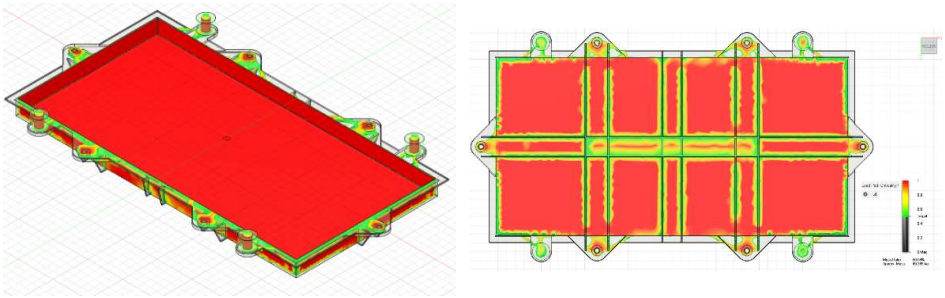

Figure 14

iv) Generative Design

A generative design was set up with absolutely necessarily parts; these are the battery tray, the location pins (red circle) and bolt attaching points (green circle) (Figure 15). Fixed constraints are defined where the bolts will be attaching the battery tray to the underbody of the car. The 6 load cases are also used to determine the shape.

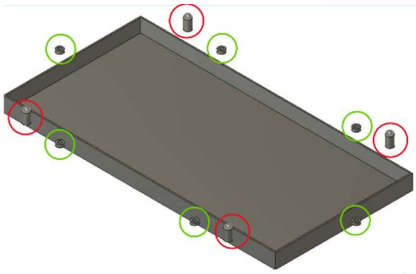

Figure 15

Below are some of the generative outcomes (Figure 16):

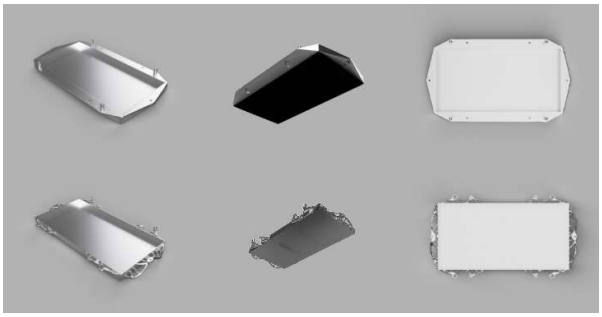

Figure 16

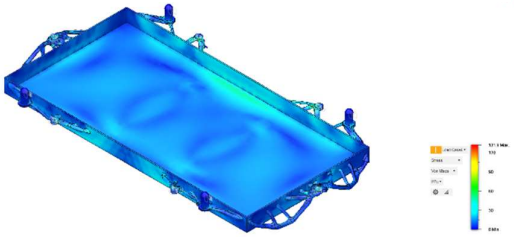

Figure 17

The retest of design obtained through the generative design (Figure 17) shows that the design can handle all 6 load cases with ease (**highest stress at 131.9MPa**), scoring **minimum safety factor of 1.99**, while being the lightest of all designs thus far. However, some geometries of the design must be simplified further to improve the stress path.

5) <u>Design Conclusion</u>

In conclusion, the **2nd design iteration made of wrought magnesium alloy** will be selected over the generative designs as the final product (Figure 18). This is due to shape simplicity, which is easier to be manufactured via forging. This expensive method further requires a secondary shaping process to improve the accuracy of the design, which only adds more cost to manufacture. This can also be difficult to be mass-produced if more steps are involved.

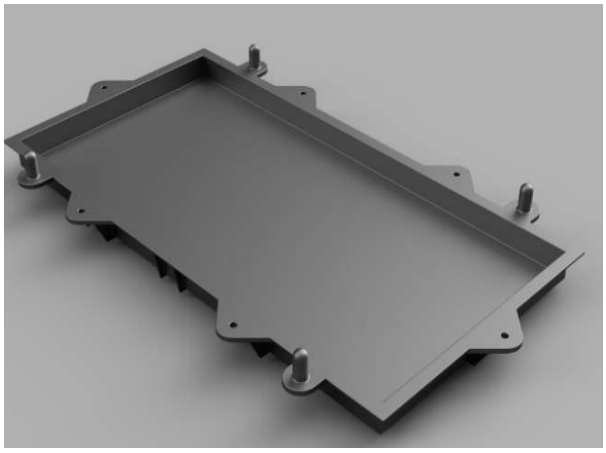

Figure 18 final design

Furthermore, the final product has a minimum safety factor of 2.91, which is 46 percent higher than that of the generative designs with a value of 1.99. This is essential to fulfill the function of the tray that it must provide maximum safety not just passing the safety requirement. However, the drawback comes with a heavier net mass of the design of 62.5 kg, which is 7 kg heavier than that of the generative design due to excess material that would bear no load under normal circumstances but provide further support under outlying and unpredictable factors.

References

Maddock, B. (2020, April 8). *Passenger Turning Path - 180°*. Retrieved from Dimensions: https://www.dimensions.com/element/passenger-vehicle-180-degree-turning-paths-radius

McMaster-Carr. (2021). *Alloy Steel Thread-Locking Socket Head Screws*. Retrieved from McMaster-Carr: https://www.mcmaster.com/thread-locking-socket-head-cap-screws/alloy-steel-thread-locking-socket-head-screws/

Porsche AG. (2021). *Porsche*. Retrieved from Taycan Turbo S: https://www.porsche.com/international/models/taycan/taycan-models/taycan-turbo-s/

Racing Circuits. (2021). *Bristol Motor Speedway*. Retrieved from racingcircuits: https://www.racingcircuits.info/north-america/usa/bristol-motor-speedway.html#.YABEkuj7RPY

Statista Research Department. (2021, January 11). *Electricity prices for households in the United Kingdom (UK) 2010-2020, semi-annually*. Retrieved from Statista: https://www.statista.com/statistics/418126/electricity-prices-for-households-in-the-uk/

Appendix

MPI derivations

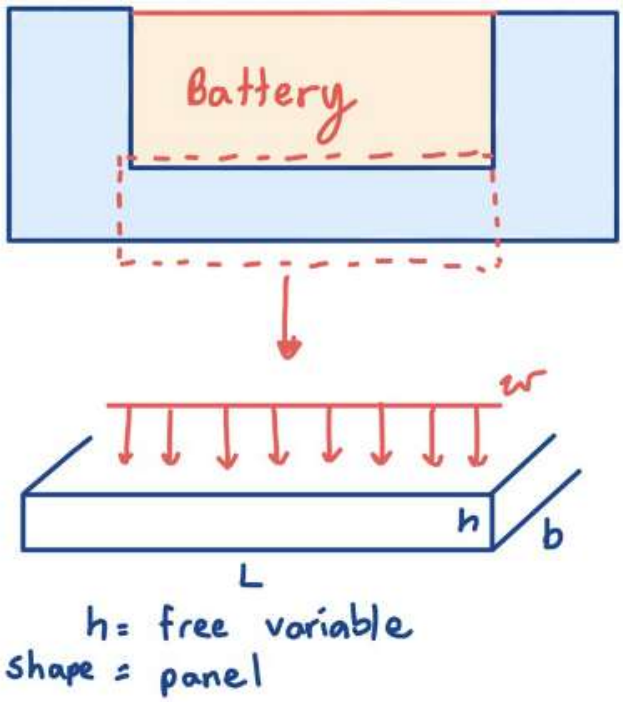

The lower part of the tray is used for the MPI derivations. The tray is assumed to be a panel with a uniformly distributed force, w, acting on it.

MPIs strength and mass

$$Mass = Lhb\rho$$

$$F_f = \frac{16I\sigma_{max}}{h_{max}\,L}$$

$$I = \frac{bh^3}{12}$$

$$F_f = \frac{16\frac{bh^3}{12}\sigma_{max}}{\frac{h}{2}\,L}$$

$$F_f = \frac{8bh^2\sigma_{max}}{3\,L}$$

$$h = \left(\frac{3F_fL}{8\,b\sigma_{max}}\right)^{0.5}$$

$$Mass = L\left(\frac{3F_fL}{8\,b\sigma_{max}}\right)^{0.5} b\rho$$

$$MPI = \frac{{\sigma_{max}}^{0.5}}{\rho}$$

MPIs strength and cost

C_m = cost per unit mass

$$Cost = Lhb\rho C_m$$

$$F_f = \frac{16I\sigma_{max}}{h_{max}\,L}$$

$$I = \frac{bh^3}{12}$$

$$F_f = \frac{16\frac{bh^3}{12}\sigma_{max}}{\frac{h}{2}\,L}$$

$$F_f = \frac{8bh^2\sigma_{max}}{3\,L}$$

$$h = \left(\frac{3F_fL}{8\,b\sigma_{max}}\right)^{0.5}$$

$$Cost = L\left(\frac{3F_fL}{8\,b\sigma_{max}}\right)^{0.5} b\rho C_m$$

$$MPI = \frac{{\sigma_{max}}^{0.5}}{\rho C_m}$$

MPIs stiffness and mass

$$Mass = Lhb\rho$$

$$S = \frac{C_1 EI}{L^3}$$

$$I = \frac{bh^3}{12}$$

$$S = \frac{C_1 E \frac{bh^3}{12}}{L^3}$$

$$h = \left(\frac{12S}{C_1 Eb}\right)^{\frac{1}{3}} L$$

$$Mass = \left(\frac{12Sb^2}{C_1}\right)^{\frac{1}{3}} L^2 \left(\frac{\rho}{E^{\frac{1}{3}}}\right)$$

$$MPI = \frac{E^{\frac{1}{3}}}{\rho}$$

MPIs stiffness and cost

$$Cost = Lhb\rho C_m$$

$$S = \frac{C_1 EI}{L^3}$$

$$I = \frac{bh^3}{12}$$

$$S = \frac{C_1 E \frac{bh^3}{12}}{L^3}$$

$$h = \left(\frac{12S}{C_1 Eb}\right)^{\frac{1}{3}} L$$

$$Cost = \left(\frac{12Sb^2}{C_1}\right)^{\frac{1}{3}} L^2 \left(\frac{\rho}{E^{\frac{1}{3}}}\right) C_m$$

$$MPI = \frac{E^{\frac{1}{3}}}{\rho C_m}$$

MPIs fatigue strength and mass

$$Mass = Lhb\rho$$

$$\frac{wL}{\sigma_f} = bh$$

$$\frac{wL}{\sigma_f b} = h$$

$$Mass = L\frac{wL}{\sigma_{fb} b} b\rho$$

$$Mass = L^2 w \frac{\rho}{\sigma_f}$$

$$MPI = \frac{\sigma_f}{\rho}$$

MPIs fatigue strength and mass and cost

$$Cost = Lhb\rho C_m$$

$$\frac{wL}{\sigma_f} = bh$$

$$\frac{wL}{\sigma_f b} = h$$

$$Cost = L\frac{wL}{\sigma_{fb} b} b\rho C_m$$

$$Cost = L^2 w \frac{\rho}{\sigma_f} C_m$$

$$MPI = \frac{\sigma_f}{\rho C_m}$$

Load case calculations:

$m_B = 350\ kg$, $g = 9.81\ ms^{-2}$, $\alpha = 22^\circ$, $V = 260\ km/h = \frac{650}{9}\ ms^{-1} = 72.2\ ms^{-1}$, $R = 10.7$ meters.

① Tray: $N_{BT} = m_B g$
Bolts: $R_{Ty} = N_{BT} + m_T g$

$N_{BT} = 350(9.81) = 3433.5\ N$
$N_{Bx} = 0\ N$

② Tray – Y: $N_{BTy} = m_B g \cos\alpha$
Tray – X: $N_{BTx} = m_B g \sin\alpha$
Bolts – Y: $R_{Ty} = N_{BTy} + m_T g \cos\alpha$
Bolts – X: $R_{Tx} = N_{BTx} + m_T g \sin\alpha$.

$N_{BTy} = 350(9.81)\cos 22^\circ = 3183.5\ N$
$N_{BTx} = 350(9.81)\sin 22^\circ = 1286.2\ N$

③ Tray – Y: $N_{BTy} = m_B g$
Tray – X: $N_{BTx} = m_B a_{Bx}$
Bolts – Y: $R_{Ty} = N_{BT} + m_T g$
Bolts – X: $R_{Tx} = m_T a_{Tx} + N_{BTx}$

$N_{BTy} = 3433.5\ N$
$N_{BTx} = 350(11.6) = 4060\ N$

④ Tray – Y: $N_{BTy} = m_B g \cos\alpha$
Tray – X: $N_{BTx} = m_B g \sin\alpha + m_B a_{Bx}$
Bolts – Y: $R_{Ty} = N_{BTy} + m_T g \cos\alpha$
Bolts – X: $R_{Tx} = N_{BTx} + m_T g \sin\alpha$

$N_{BTy} = 350(9.81)\cos 22^\circ = 3183.5\ N$
$N_{BTx} = 350(9.81)\sin 22^\circ + 350(11.6) = 5346.2\ N$

⑤ 40 km/h

Tray – Y: $N_{BTy} = m_B g$

Tray – X: $N_{BTx} = m_B a_{Bn} = m_B \left(\frac{V^2}{R}\right)$

Bolts – Y: $R_{Ty} = N_{BTy} + m_T g$

Bolts – X: $R_{Tx} = N_{BTx} + m_T \left(\frac{V^2}{R}\right)$

$N_{BTy} = 3433.5\ N$

$N_{BTx} = 4038.3\ N$

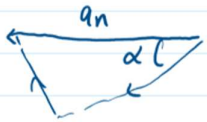

⑥ use 150 km/h

Tray – Y: $N_{BTy} = m_B g \cos\alpha + m_B a_{Bn} \sin\alpha$

Tray – X: $N_{BTx} = m_B g \sin\alpha - m_B a_{Bn} \cos\alpha$

Bolts – Y: $R_{Ty} = m_T a_T \sin\alpha + N_{BTy} + m_T g \cos\alpha$

Bolts – X: $R_{Tx} = m_T a_T \cos\alpha - N_{BTx} - m_T g \sin\alpha$

$N_{BTy} = 350(9.81)\cos 22° + 350\left(\frac{V^2}{10.7}\right)\sin 22° = 24456.9\ N$

$N_{BTx} = 350(9.81)\sin 22° - 350\left(\frac{V^2}{10.7}\right)\cos 22° = -51367.3\ N$